Machine Copy for Proofreading, Vol. x, y–z, 2012

A TRANS-IMPEDANCE GREEN'S FUNCTION FOR THE DIELECTRIC RING CIRCULATOR

R. S. Adams* **and A. K. Hatley**

Department of Electrical and Computer Engineering, University of North Carolina Charlotte, Charlotte, North Carolina, 9201 University City Blvd, Charlotte, NC 28223, USA

Abstract—An efficient trans-impedance Green's function that describes the electromagnetic behavior of a ring circulator is presented. A rigorous derivation comprised of an infinite summation of modified Bessel functions of the first and second kinds is included. As with more traditional circulator descriptions, the formulation herein contains a weak singularity when the measurement point is located near the impressed source point on the same radius. To accelerate convergence of the series, this singularity is extracted from the formulation and integrated analytically. To complete the formulation, two circulators are presented; the first with ports that emanate at equal angles from the outer radius, and the second with two ports associated with the outer radius and one port that connects to the inner radius. The computation time associated with the proposed analysis lasted approximately 0.25 s, whereas an identical structure simulated via a common full-wave solver lasted approximately 10 hours. Comparison of impedance data between the proposed analysis and full-wave simulation is presented.

1. INTRODUCTION

Microwave ferrite circulators are enabling technologies in monostatic RADAR and critical communication systems. They were experimentally demonstrated by Schaug and Pettersen in 1957 [1] and have been the subject of active investigation both experimentally and theoretically ever since. The first accurate, theoretical, electromagnetic description of these devices was presented by Bosma in 1964 [2] with further analyses by many such as Fay and Comstock [3], Wu and Rosenbaum [4], and Young and Johnson [5].

Received 10 August 2012.

* Corresponding author: Ryan S. Adams (radams41@uncc.edu).

Modifications to the structure of the traditional circulator have led to devices such as waveguide circulators [6], slotline circulators [7], and ferrite coupled line (FCL) circulators [8]. One other topology that was suggested by Davis et. al., is the ferrite ring circulator [9]. This device was initially described conceptually, and an approximate preliminary analysis was presented. Although this geometry was discussed in the context of a Green's function by Krowne and Neidert [10], their analysis did not allow inner ports.

The ring circulator holds appeal since it allows additional space in the center of the device where antennas, amplifiers, etc. may be placed. Also, such devices provide isolation of the inner port signals from any substrate modes that are present on the outside of the circulator due to the attenuation of the ferrite ring itself. These advantages have led to the desire for a computationally efficient electromagnetic description for the ferrite ring circulator that may be used to design optimal devices for specific applications. Such an explanation will provide insight into optimal choices for inner and outer radius, material properties, etc..

In the ensuing sections, the basic Green's function will be derived, followed by a modification that improves convergence through extraction of an asymptotic singularity that is present in the basic description. The paper concludes with presentation of two distinct circulator designs: one with ports entirely connected to the outer radius; the other circulator was designed with a single port connected to the inner radius and the remaining two ports connected to the outer radius. These two designs are presented to demonstrate the functionality of an inner port; two and three inner ports are equally supported. Comparison of Green's function and simulation data from a full-wave solver are included for both designs.

2. FORMULATION

Electric and magnetic fields within a fully saturated ferrite material satisfy Maxwell's equations. Since no permanent electric dipole moment exists in most ferrite materials, the relationship between $\mathbf{E}$ and $\mathbf{D}$ is defined by the traditional electric field constitutive relation, or $\mathbf{D} = \epsilon\mathbf{E}$; however, the presence of permanent magnetic dipole moments cause the relationship between $\mathbf{B}$ and $\mathbf{H}$ to depend on the direction of propagation. To account for this directional dependence, the relationship between $\mathbf{B}$ and $\mathbf{H}$ is expressed in the form of a tensor first proposed by Polder [11]. When the magnetic bias is z-directed,

Maxwell's equations are expressed as

$$\nabla \times \mathbf{E} = -\begin{bmatrix} \mu & j\kappa & 0 \\ -j\kappa & \mu & 0 \\ 0 & 0 & \mu_\circ \end{bmatrix} \frac{\partial \mathbf{H}}{\partial t} \tag{1}$$

$$\nabla \times \mathbf{H} = \epsilon_\circ \epsilon_r \frac{\partial \mathbf{E}}{\partial t} \tag{2}$$

Here μ and κ depend on material properties as well as the frequency of operation.

It is not the purpose of this effort to develop a perfect description that accounts for every aspect of the electromagnetic problem associated with a ring circulator. Rather, it is our intent to present an approximate equation that is sufficiently accurate to give meaningful

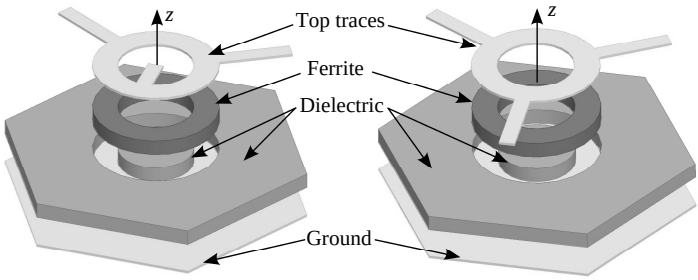

Figure 1. Geometrical and material structure of candidate ring circulators. Note that $z = 0$ is located coincident with the ground plane.

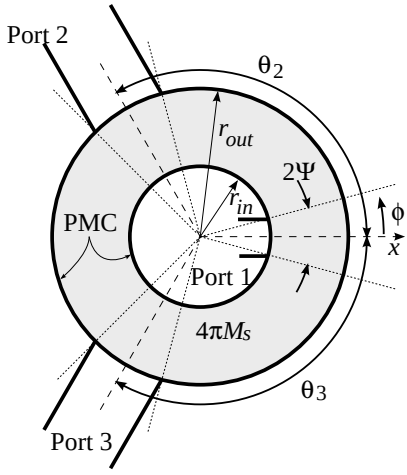

Figure 2. Proposed computational structure.

results, but with computational efficiency to be useful as the kernel of an appropriate design algorithm. With this philosophy in mind, the geometry of Figure 1 is assumed to be bounded by Perfect Electric Conductors (PEC) on the top and bottom faces (i.e., $z = 0, h$) and with Perfect Magnetic Conductor (PMC) boundaries on the inner and outer ring surfaces. These and other geometrical definitions are described in Figure 2. These boundary conditions lead naturally to TM_z solutions where $E_r = E_\phi = H_z = 0$. To simplify the analysis further, it is assumed that the device is very thin (i.e., h: small), so all derivatives with respect to z are negligible. With these assumptions, Equations (1)–(2) simplify to three scalar equations

$$H_r = \frac{1}{\omega\mu_e}\left[\frac{j}{r}\frac{\partial E_z}{\partial \phi} - \frac{\kappa}{\mu}\frac{\partial E_z}{\partial r}\right] \tag{3}$$

$$H_\phi = -\frac{1}{\omega\mu_e}\left[\frac{\kappa}{\mu r}\frac{\partial E_z}{\partial \phi} + j\frac{\partial E_z}{\partial r}\right] \tag{4}$$

and

$$\frac{1}{r}\frac{\partial}{\partial r}\left(r\frac{\partial E_z}{\partial r}\right) + \frac{1}{r^2}\frac{\partial E_z}{\partial \phi^2} + k^2 E_z = 0 \tag{5}$$

where $\mu_e = (\mu^2 - \kappa^2)/\mu$ is the effective permeability and $k^2 = \omega^2\mu_e\epsilon$ is the wavenumber associated with the electromagnetic wave.

The solution for Equation (5) consists of two linearly independent solutions in ϕ and two linearly independent solutions in r. However, since the device has rotational symmetry, the final solution must repeat every 2π so only one ϕ directed solution is necessary. So, the general solution for E_z may be expressed as

$$E_z = \sum_{n=-\infty}^{\infty} \left[A_n I_n(\gamma r) + B_n K_n(\gamma r)\right] e^{jn\phi} \tag{6}$$

where $\gamma = jk$, and I_n, K_n are the modified Bessel functions of the first and second kinds, respectively; A_n and B_n are coefficients to be determined. Equation (6) may be used with Equation (4) to yield the following general equation for H_ϕ

$$\begin{aligned} H_\phi = & -\frac{j\gamma}{\omega\mu_e}\sum_{n=-\infty}^{\infty}\left[A_n I_n'(\gamma r) + B_n K_n'(\gamma r)\right] e^{jn\phi} \\ & -\frac{j\kappa}{\omega\mu_e\mu r}\sum_{n=-\infty}^{\infty} n\left[A_n I_n(\gamma r) + B_n K_n(\gamma r)\right] e^{jn\phi} \end{aligned} \tag{7}$$

To develop the Green's function, an azimuthally directed magnetic field is impressed at a source point on one of the PMC surfaces. Let the

source radius be $r = a_s$ and source angle be $\phi = \phi_s$, so the azimuthal component of $\mathbf{H}$ is given by

$$H_\phi = H_\circ \delta(\phi - \phi_s) \tag{8}$$

This equation represents a periodic function in ϕ with fundamental period $T_\circ = 2\pi$. Any such function can be expanded in a Fourier series according to

$$H_\phi = \frac{H_\circ}{2\pi} \sum_{n=-\infty}^{\infty} e^{jn(\phi-\phi_s)} \tag{9}$$

Uniqueness assures that Equations (7) and (9) are identical descriptions for H_ϕ. A term-by-term equality of these two equations gives rise to the following

$$\begin{aligned} \frac{H_\circ}{2\pi} e^{-jn\phi_s} &= -\frac{j\gamma}{\omega\mu_e}\left[A_n I_n'(\gamma a_s) + B_n K_n'(\gamma a_s)\right] \\ &\quad -\frac{j\kappa n}{\omega\mu_e\mu a_s}\left[A_n I_n(\gamma a_s) + B_n K_n(\gamma a_s)\right] \end{aligned} \tag{10}$$

Here, the PMC boundary condition is enforced everywhere on the source surface except at the source point. However, since more than one PMC surface exists in the proposed structure, an additional boundary condition must be applied. To enforce the PMC boundary on the non-source surface, let $r = a_\circ$ be the radius of the surface with no source present. On this surface, H_ϕ must be forced to zero everywhere. This requirement is satisfied if

$$B_n = -A_n \left[\frac{\gamma I_n'(\gamma a_\circ) + \frac{n\kappa}{\mu a_\circ} I_n(\gamma a_\circ)}{\gamma K_n'(\gamma a_\circ) + \frac{n\kappa}{\mu a_\circ} K_n(\gamma a_\circ)}\right] \tag{11}$$

Equations (10) and (11) represent two linearly independent equations that may be used to solve for the coefficients A_n and B_n of Equation (6). To simplify the formulation, the constant $H_\circ$ and the phase terms are removed from the coefficients (i.e., $A_n = A_{n\circ} H_\circ e^{-jn\phi_s}$ and $B_n = B_{n\circ} H_\circ e^{-jn\phi_s}$) and the first modified coefficient term is given by

$$A_{n\circ} = \frac{\Lambda_n(a_\circ)\left(j\frac{\omega\mu_e}{2\pi}\right)}{\Lambda_n(a_\circ)\Psi_n(a_s) - \Lambda_n(a_s)\Psi_n(a_\circ)} \tag{12}$$

where the intermediate functions $\Lambda_n(x)$ and $\Psi_n(x)$ are given by

$$\Lambda_n(x) = \frac{n\kappa_f}{\mu_f x} K_n(\gamma_f x) + \gamma_f K_n'(\gamma_f x) \tag{13}$$

$$\Psi_n(x) = \frac{n\kappa_f}{\mu_f x} I_n(\gamma_f x) + \gamma_f I_n'(\gamma_f x) \tag{14}$$

Similarly, the second modified coefficient term is given by

$$B_{n\circ} = -\frac{\Psi_n(a_\circ)\left(j\frac{\omega\mu_e}{2\pi}\right)}{\Lambda_n(a_\circ)\Psi_n(a_s) - \Lambda_n(a_s)\Psi_n(a_\circ)} \tag{15}$$

Thus, the z-directed electric field at the arbitrary location r, ϕ is deduced from

$$E_z = \sum_{n=-\infty}^{\infty} \left[A_{n\circ} I_n(\gamma r) + B_{n\circ} K_n(\gamma r)\right] H_\circ e^{jn(\phi-\phi_s)} \tag{16}$$

where the coefficients $A_{n\circ}$ and $B_{n\circ}$ are given in Equations (12) and (15).

To determine the electric field at an arbitrary point due to a source across a port of finite length, Equation (16) must be integrated across the source port. This resulting equation becomes a trans-impedance Green's function when the magnitude of the impressed magnetic field is divided out of the resulting integral equation. If the excitation port is port j, the measurement port is port i, and the width of the excitation port is defined by ψ_j, then the impedance parameters associated with this three port structure are expressed as

$$Z_{ij} = \frac{E_z}{H_\circ} = \int_{\phi_j-\psi_j}^{\phi_j+\psi_j} G\left(r_i, \phi_i; r', \phi'\right) d\phi' \tag{17}$$

Here $G(r_i, \phi_i; r', \phi')$ is the trans-impedance Green's function and is given by

$$G\left(r_i, \phi_i; r', \phi'\right) = G_\circ + G_1 + G_2 \tag{18}$$

where

$$G_\circ = A_{0\circ} I_0(\gamma_f a_i) + B_{0\circ} K_0(\gamma_f a_i) \tag{19}$$

$$G_1 = \sum_{n=1}^{\infty} \left[A_{n\circ} I_n(\gamma_f a_i) + B_{n\circ} K_n(\gamma_f a_i)\right] e^{jn(\phi_i-\phi')} \tag{20}$$

$$G_2 = \sum_{n=-1}^{-\infty} \left[A_{n\circ} I_n(\gamma_f a_i) + B_{n\circ} K_n(\gamma_f a_i)\right] e^{jn(\phi_i-\phi')} \tag{21}$$

According to the standard definition of impedance parameters, the current at each port is defined to be entering the network. Thus, Equation (17) computes the impedance parameters associated with an exterior excitation port; interior excitation ports require a negative sign multiplying Equation (17) to reverse the direction of port current. Equivalently, the direction of integration of Equation (17) should be reversed when inner ports are treated as the source.

3. SINGULARITY EXTRACTION

It has been observed that the Green's function above contains a weak singularity when the measurement angle approaches the source angle on the source radius; no singularity is observed when measuring fields on the non-source radius. This singularity does not prevent arrival at the desired solution; however, the singularity requires that an unreasonably large number of terms in the infinite sums of Equations (20) and (21) be used to arrive at an accurate solution. To accelerate convergence of this function, the singularity is isolated in closed form and computed separately [12].

Since the singularity only exists on the radius where the source is impressed, a_s, this radius will be used in the singularity extraction process. To isolate the singularity, Equations (13) and (14) are rewritten as

$$\Lambda_n(x) = \frac{n}{x}\left(\frac{\kappa_f}{\mu_f}+1\right)K_n(\gamma_f x) - \gamma_f K_{n+1}(\gamma_f x) \tag{22}$$

$$\Psi_n(x) = \frac{n}{x}\left(\frac{\kappa_f}{\mu_f}+1\right)I_n(\gamma_f x) + \gamma_f I_{n+1}(\gamma_f x) \tag{23}$$

where the identities

$$\frac{dI_n(x)}{dx} = \frac{n}{x}I_n(x) + I_{n+1}(x) \tag{24}$$

$$\frac{dK_n(x)}{dx} = \frac{n}{x}K_n(x) - K_{n+1}(x) \tag{25}$$

were used [13]. Equations (22) and (23) are combined with (12) and (15) to form the relation $A_{n\circ}I_n(\gamma_f a_s) + B_{n\circ}K_n(\gamma_f a_s)$. The numerator of this equation is

$$\begin{aligned}\text{Num} = {} & \frac{j\omega\mu_e n}{2\pi a_\circ}\left[\frac{\kappa_f}{\mu_f}+1\right]\left[K_n(\gamma_f a_\circ)I_n(\gamma_f a_s) - I_n(\gamma_f a_\circ)K_n(\gamma_f a_s)\right] \\ & -\frac{j\omega\mu_e\gamma}{2\pi}\left[K_{n+1}(\gamma_f a_\circ)I_n(\gamma_f a_s) - I_{n+1}(\gamma_f a_\circ)K_n(\gamma_f a_s)\right]\end{aligned} \tag{26}$$

and the denominator is

$$\begin{aligned}\text{Den} = {} & \frac{n^2}{a_\circ a_s}\left(\frac{\kappa_f}{\mu_f}+1\right)^2\left[K_n(\gamma_f a_\circ)I_n(\gamma_f a_s) - K_n(\gamma_f a_s)I_n(\gamma_f a_s)\right] \\ & +\frac{n\gamma_f}{a_\circ}\left(\frac{\kappa}{\mu}+1\right)\left[K_n(\gamma_f a_\circ)I_{n+1}(\gamma_f a_s) + K_{n+1}(\gamma_f a_s)I_n(\gamma_f a_\circ)\right] \\ & -\frac{n\gamma_f}{a_s}\left(\frac{\kappa_f}{\mu_f}+1\right)\left[K_{n+1}(\gamma_f a_\circ)I_n(\gamma_f a_s)+K_n(\gamma_f a_s)I_{n+1}(\gamma_f a_\circ)\right] \\ & +\gamma^2\left[K_{n+1}(\gamma_f a_s)I_{n+1}(\gamma_f a_\circ) - K_{n+1}(\gamma_f a_\circ)I_{n+1}(\gamma_f a_s)\right]\end{aligned} \tag{27}$$

In the limit as $n \to +\infty$, the numerator and denominator simplify to

$$\lim_{n\to+\infty}\{\text{Num}\} = \left(\frac{j\omega\mu_e}{2\pi}\right)\left(\frac{n}{a_\circ}\right)\left[\frac{\kappa_f}{\mu_f}+1\right][K_n(\gamma_f a_\circ)I_n(\gamma_f a_s) - I_n(\gamma_f a_\circ)K_n(\gamma_f a_s)] \tag{28}$$

and

$$\lim_{n\to+\infty}\{\text{Den}\} = \frac{n^2}{a_\circ a_s}\left(\frac{\kappa_f}{\mu_f}+1\right)^2[K_n(\gamma_f a_\circ)I_n(\gamma_f a_s) - K_n(\gamma_f a_s)I_n(\gamma_f a_s)] \tag{29}$$

respectively. The ratio of numerator and denominator leads to the limiting case

$$\lim_{n\to+\infty}\{A_{n\circ}I_n(\gamma_f a_s)+B_{n\circ}K_n(\gamma_f a_s)\} = \frac{a_s}{n\left(1+\frac{\kappa_f}{\mu_f}\right)}\frac{j\omega\mu_e}{2\pi} \tag{30}$$

In a similar fashion,

$$\lim_{n\to-\infty}\{A_{n\circ}I_n(\gamma_f a_s)+B_{n\circ}K_n(\gamma_f a_s)\} = \frac{a_s}{n\left(1-\frac{\kappa_f}{\mu_f}\right)}\frac{j\omega\mu_e}{2\pi} \tag{31}$$

To remove the asymptotic singularity from the Green's function of Equation (18) the following form is employed

$$G\left(r_i,\phi_i;r',\phi'\right) = G_\circ + G_{1a} + G_{2a} + G_a \tag{32}$$

where $G_\circ$ is given by Equation (19), G_{1a}, G_{2a}, are modified from Equations (20) and (21) by subtraction of the asymptotic terms of Equations (30) and (31); G_a represents the addition of the asymptotic terms. These three terms are given by

$$G_{1a} = \sum_{n=1}^{\infty}\left[A_{n\circ}I_n(\gamma_f a_i)+B_{n\circ}K_n(\gamma_f a_i) - \frac{a_s j\omega\mu_e}{2\pi n\left(1+\frac{\kappa_f}{\mu_f}\right)}\right]e^{jn(\phi_i-\phi')} \tag{33}$$

$$G_{2a} = \sum_{n=-1}^{-\infty}\left[A_{n\circ}I_n(\gamma_f a_i)+B_{n\circ}K_n(\gamma_f a_i) - \frac{a_s j\omega\mu_e}{2\pi n\left(1-\frac{\kappa_f}{\mu_f}\right)}\right]e^{jn(\phi_i-\phi')} \tag{34}$$

$$G_a = \frac{j\omega\mu_e a_s}{2\pi}\left[\sum_{n=-1}^{-\infty}\frac{e^{jn(\phi_i-\phi')}}{n\left(1-\frac{\kappa_f}{\mu_f}\right)} + \sum_{n=1}^{\infty}\frac{e^{jn(\phi_i-\phi')}}{n\left(1+\frac{\kappa_f}{\mu_f}\right)}\right] \tag{35}$$

To accelerate convergence of the overall Green's function of Equation (32), the infinite summations of Equation (35) are replaced

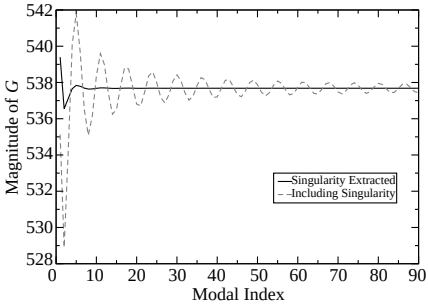

Figure 3. Comparison of convergence of $G(a_s, \phi_i; a_s, \phi')$ as calculated by Equations (18) and (32) for $\phi_i - \phi' = 1.0\,\text{rad}$.

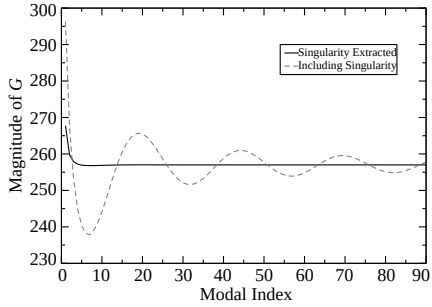

Figure 4. Comparison of convergence of $G(a_s, \phi_i; a_s, \phi')$ as calculated by Equations (18) and (32) for $\phi_i - \phi' = 0.25\,\text{rad}$.

with their equivalent analytical expressions [13]. These expressions are proportional to the natural logarithm of complex argument [13] according to

$$G_a = -\frac{j\omega\mu_e a_s}{2\pi}\left[\frac{\ln\left(1-e^{-j(\phi_i-\phi')}\right)}{\left(1-\frac{\kappa_f}{\mu_f}\right)} + \frac{\ln\left(1-e^{j(\phi_i-\phi')}\right)}{\left(1+\frac{\kappa_f}{\mu_f}\right)}\right] \tag{36}$$

Thus, the modified Green's function of Equation (32), with G_{1a}, G_{2a} and G_a described by Equations (33), (34) and (36) respectively, is used to describe the behavior of the ferrite ring circulator of Figure 2.

This modified Green's function converges much more rapidly than the basic Green's function of Equation (18), particularly for small values of $\phi_i - \phi'$. To illustrate this acceleration of convergence, consider a circulator with outer radius $r_{out} = 2\,\text{mm}$, $r_{in} = 0.6\,\text{mm}$, $4\pi M_s = 1000\,\text{Gauss}$, $\Delta H = 120\,\text{Oe}$, $\epsilon_r = 11.6$, $H_\circ = 0\,\text{Oe}$, and operating frequency $f = 11\,\text{GHz}$. The Green's function evaluated a distance $\phi_i - \phi' = 1.0\,\text{rad}$ away from the source is shown in Figure 3 for the Green's function forms outlined in Equations (18) and (32). Similarly, Figure 4 shows comparison of the two forms of the Green's function for a distance of $\phi_i - \phi' = 0.25\,\text{rad}$. These figures demonstrate that as radial distance narrows, the number of terms required to assure convergence grows for the Green's function of Equation (18), but Equation (32) does not.

4. NUMERICAL RESULTS

To validate the Green's function presented above, two circulators were designed and simulated, one with three ports at equal intervals around

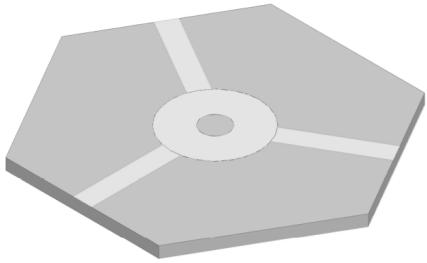

Figure 5. The simulated geometry of design 1 with three ports emanating from the outer radius an equal distance apart ($\theta_2 = \theta_3 = 2\pi/3$).

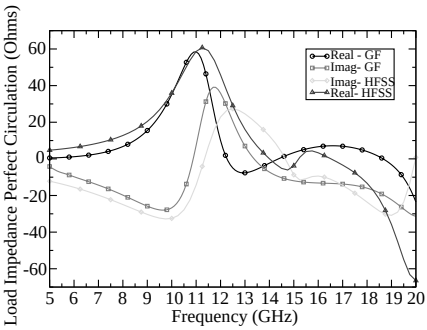

Figure 6. A comparison of load impedance for perfect circulation from [14] for the first design calculated with Green's function of Equation (32) and simulated by HFSS.

the outer surface of the ferrite ring, and the other with two ports about the outer edge and a single port on the inner radius. Good correlation is observed with both designs. These two designs were chosen to demonstrate validity under multiple configurations.

To evaluate the quality of a given design, it is often easier to express the circulator response in terms of the load impedance for perfect circulation [14]. A circulator described in this manner may be easily evaluated in terms of its matchability for a given criteria. Although the Bode-Fano criterion may be exceeded with these impedances, it still may be applied to provide a good rule of thumb regarding matchability of a given three port circulator. When rotational symmetry is not present, the impedance is unique for each port, and thus three distinct impedances may be necessary to fully characterize a device.

The first circulator design consists of a ferrite ring with three identical ports a uniform $2\pi/3$ apart, as shown in Figure 5. Using the Green's function described above, the following geometrical parameters were determined: inner radius $a_{in} = 0.6\,\text{mm}$, outer radius $a_{out} = 2.0\,\text{mm}$, coupling angle $\psi = 12°$, and dielectric thickness $d = 0.5\,\text{mm}$. The circulator used ferrite material with $4\pi M_s = 1000\,\text{Gauss}$, $\Delta H = 120\,\text{Oe}$, $\epsilon_r = 11.6$, internal field $H_\circ = 0$, and surrounding dielectric material with relative permittivity $\epsilon_d = 20$. Comparison of the Green's function of Equation (32) and simulated data from HFSS is presented in Figure 6 which shows the computed load impedance for perfect circulation as presented in [14]. Deviation of the Green's function from the results of HFSS consist of primarily a small magnitude shift due to fringing of the microstrip structure.

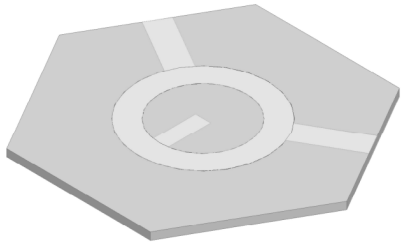

Figure 7. The simulated geometry of design 2 with port one emanating from the inner radius and the remaining two ports emanating from the outer radius; all ports are an equal radial distance apart ($\theta_2 = \theta_3 = 2\pi/3$).

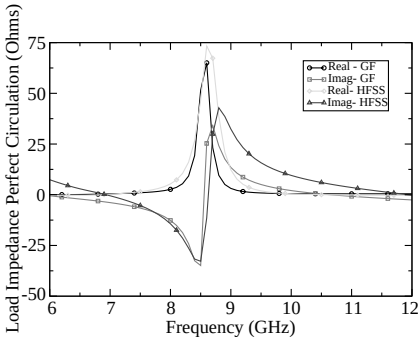

Figure 8. A comparison of load impedance for perfect circulation from [14] for the inner port of the second design calculated with Greens function of Equation (32) and simulated by HFSS.

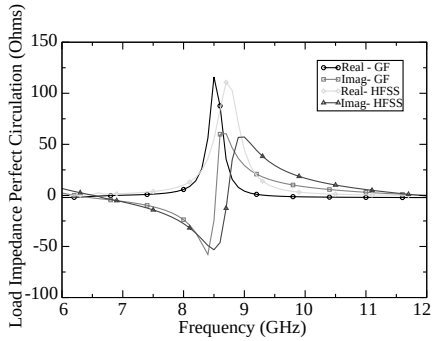

Figure 9. A comparison of load impedance for perfect circulation from [14] for the outer ports of the second design calculated with Green's function of Equation (32) and simulated by HFSS.

The second circulator design was chosen to demonstrate circulation with a single port on the inner radius of the circulator and is shown in Figure 7. This device represents a fundamental shift in behavior from the traditional circulator described by Bosma [2] in that energy is routed through the center of the device, rather than along the outer edge. All ports emanate from the ferrite region at equal angles of $2\pi/3$; the Green's function described above suggested the following geometrical parameters for good performance: inner radius $a_{in} = 3.0\,\text{mm}$, outer radius $a_{out} = 4.5\,\text{mm}$, coupling angle $\psi = 10°$, and dielectric thickness $d = 0.5\,\text{mm}$. The circulator uses ferrite material with $4\pi M_s = 500\,\text{Gauss}$, $\Delta H = 190\,\text{Oe}$, $\epsilon_r = 9.0$, internal field $H_\circ = 0$, and surrounding dielectric material with relative permittivity

$\epsilon_d = 25$. Because of the lack of rotational symmetry, comparison of the Green's function of Equation (32) and simulated data from HFSS must include the load impedances for perfect circulation from port 1 as well as from ports 2 and 3; the impedances associated with ports 2 and 3 are identical. These data are presented in Figures 8 and 9. As with design 1, deviation of the Green's function from HFSS consists of primarily a small magnitude shift primarily due to fringing of the microstrip structure. It should be noted that the time required to compute the Green's function for both designs was approximately 0.25 s using a single processor; whereas, the time required to compute the port response using a full-wave electromagnetic solver (HFSS) was approximately 10 hours using approximately 6 processors in a parallel configuration.

5. CONCLUSION

A trans-impedance Green's function for a microstrip ring circulator is presented. To accelerate convergence of the infinite sums associated with the Green's function, an asymptotic analysis is accomplished wherein the singularity is removed and computed analytically. The goal of computational efficiency is verified in that the time to compute the Green's function is approximately 0.25 s as compared with the time to compute the full-wave solution is approximately 10 hours. Feasibility of a circulator with one or more ports on the interior of the device was demonstrated. This geometrical configuration provides functionality that has not previously been considered for circulator devices. For example, a relatively large ring circulator with all ports on the interior of the ferrite region could be used; all active and passive devices could be placed on the interior and the circulator could be employed in the dual roles of a nonreciprocal device, as well as a filter to remove substrate wave interaction with other parts of a substrate. These and other possibilities are natural consequences of the presented work.

ACKNOWLEDGMENT

This material is based upon work supported by the National Science Foundation under Grant No. 1028472.

REFERENCES

1. Rodrigue, G. P., "Agenerationof microwave ferrite devices," *Proc. IEEE*, Vol. 76, No. 2, 121–137, Feb. 1988.

2. Bosma, H., "On stripline y-circulation at UHF," *IEEE Trans. Microwave Theory Tech.*, Vol. 12, No. 1, 61–72, Jan. 1964.
3. Fay, C. E. and R. L. Comstock, "Operationof theferrite junction circulator," *IEEE Trans. Microwave Theory Tech.*, Vol. 13, No. 1, 15–27, Jan. 1965.
4. Wu, Y. S. and F. J. Rosenbaum, "Wide-band operation of microstrip circulators," *IEEE Trans. Microwave Theory Tech.*, Vol. 22, No. 10, 849–856, Oct. 1974.
5. Young, J. L. and C. M. Johnson, "A compact recursive trans-impedance Green's function for the inhomogeneous ferrite microwave circulator," *IEEE Trans. Microwave Theory Tech.*, Vol. 52, No. 7, 1751–1759, Jul. 2004.
6. Auld, B. A., "Thesynthesisof symmetrical waveguide circulators," *IRE Trans. Microwave Theory Tech.*, Vol. 7, 238–246, Apr. 1959.
7. Davis, L. E. and D. B. Sillars, "Millimetric nonreciprocal coupled-slot finline components," *IEEE Trans. Microwave Theory Tech.*, Vol. 34, No. 7, 804–808, 1986.
8. Teoh, C. S. and L. E. Davis, "Normal-mode analysis of ferrite-coupled lines using microstrips or slotlines," *IEEE Trans. Microwave Theory Tech.*, Vol. 43, 2991–2998, Jan. 1995.
9. Borjak, A. M. and L. E. Davis, "On planar y-ring circulators," *IEEE Trans. Microwave Theory Tech.*, Vol. 42, No. 2, 177–181, Feb. 1994.
10. Krowne, C. M. and R. E. Neidert, "Theory and numerical calculations for raidally inhomogeneous circular ferrite circulators," *IEEE Trans. Microwave Theory Tech.*, Vol. 44, No. 3, 419–431, 1996.
11. Polder, D., "On the theory of ferromagnetic resonance," *Phil. Mag.*, Vol. 40, 99, 1949.
12. Singh, S., W. F. Richards, J. R. Zinecker, and D. R. Wilton, "Accelerating theconvergence of seriesrepresenting thefreespace periodic Green's function," *IEEE Trans. Ant. Propagat.*, Vol. 38, No. 12, 1958–1962, Dec. 1990.
13. Gradshteyn, I. S. and I. M. Ryzhik, *Table of Integrals, Series, and Products,* Academic Press, Boston, MA, 2000.
14. Young, J. L., R. S. Adams, B. O'Neil, and C. M. Johnson, "Bandwidth optimization of an integrated microstrip circulator and antenna assembly: Part 2," *IEEE Antennas Propagat. Mag.*, Vol. 49, No. 1, 82–91, Feb. 2007.